مجلة جمعية الليزر العراقية
Iraqi Laser Society Journal
I.L.S.J.
Issue-2 2nd Year 2025

Increasing the Efficiency of Free-Space Optical Communication Systems Using Neural Networks

Esraa K. Al-Gazzi [1], Sawsan K. Fandi [2], and Suaad M. Ali [3]

[1, 2 and 3] Scientific Research Commission, Ministry of Higher Education and Scientific Research, Baghdad, Iraq.

Email: esraaakamil1978@gmail.com

Abstract

Weather conditions, such as dust, rain, and fog, significantly reduce the power of the laser used to transmit optical signals by altering the propagation characteristics of the light path. This degradation impacts the reliability and quality of free-space optical communication systems. This research aims primarily to develop a simple and intelligent solution to compensate for this atmospheric attenuation using a two-layer artificial neural network (ANN). Unlike conventional systems that rely on complex optical compensation mechanisms, the proposed ANN-based approach provides an efficient, less equipment-intensive alternative.

The process entails simulating various disturbance circumstances with MATLAB to simulate the behavior of genuine free-space channels. Experimenting with different attenuation levels in dust, rain, and fog conditions yields a dataset. This data is then used to train and test the neural network, which learns to forecast how much laser power is needed to maintain and improve signal integrity. The simulation program uses a 1550 nm wavelength and a 10 dB power factor to ensure accurate modeling. Key assumptions include the network's capacity to generalize attenuation patterns and recover the best power for transmission.

Keywords: Atmospheric turbulence, Optical Communication, Machine learning, and Neural Networks.

مجلة جمعية الليزر العراقية
Iraqi Laser Society Journal
I.L.S.J.
Issue-2 2nd Year 2025

زيادة كفاءة أنظمة الاتصالات البصرية في الفضاء الحر باستخدام الشبكات العصبية

اسراء كامل الغازي [1] ، سوسن خلف فندي [2] ، سعاد محمد علي [3]

هيئة البحث العلمي، وزارة التعليم العالي والبحث العلمي، بغداد، العراق[1و2و3].

Email: esraaakamil1978@gmail.com

الخلاصة

تُقلل الظروف الجوية، كالغبار والمطر والضباب، بشكل كبير من قوة الليزر المُستخدم لنقل الإشارات الضوئية، وذلك بتغيير خصائص انتشار مسار الضوء. ويؤثر هذا التدهور على موثوقية وجودة أنظمة الاتصالات الضوئية في الفضاء الحر. يهدف هذا البحث في المقام الأول إلى تطوير حل بسيط وذكي لتعويض هذا التوهين الجوي باستخدام شبكة عصبية اصطناعية (ANN) ثنائية الطبقات. وخلافًا للأنظمة التقليدية التي تعتمد على آليات تعويض ضوئية معقدة، يوفر النهج المقترح القائم على الشبكات العصبية الاصطناعية (ANN) بديلاً فعالاً وأقل استهلاكًا للمعدات.
تتضمن العملية محاكاة ظروف اضطراب مُختلفة باستخدام MATLAB لمحاكاة سلوك قنوات الفضاء الحر الحقيقية. وتُنتج تجربة مستويات توهين مُختلفة في ظروف الغبار والمطر والضباب مجموعة بيانات. تُستخدم هذه البيانات بعد ذلك لتدريب الشبكة العصبية واختبارها، والتي تتعلم التنبؤ بكمية طاقة الليزر اللازمة للحفاظ على سلامة الإشارة وتحسينها. يستخدم برنامج المحاكاة طولًا موجيًا يبلغ 1550 نانومترًا ومعامل قدرة 10 ديسيبل لضمان دقة النمذجة. تتضمن الافتراضات الرئيسية قدرة الشبكة على تعميم أنماط التوهين واستعادة أفضل طاقة للنقل.

الكلمات المفتاحية: الاضطرابات الجوية، والاتصالات البصرية، والتعلم الآلي، والشبكات العصبية.

Introduction:

Optical communication is becoming more common because it can provide a wider bandwidth than radio frequency lines and has fewer weight and power requirements. These technological benefits have made free-space optical (FSO) communication a popular method for achieving long-distance and space-based communications needs. [1] The free-space optical (FSO) communication system has recently been considered in research studies. This is because of its bandwidth, high data rate, and security in an unlicensed spectrum, as well as its easy and low-cost installation. Despite these benefits, the FSO system's applicability is limited due to its great sensitivity to weather conditions and atmospheric turbulence. [2] When a laser beam travels through a turbulent atmosphere, phase distortions build up on its wave front, which limits the link performance of free-space optical communication (FSOC) devices. Since the air path cannot be directly altered, the present efforts to enhance the physical channel's quality primarily concentrate on improving the optical transceiver's design [3]. Deep learning (DL) integration with free-space optical communications has demonstrated encouraging outcomes in terms of enhancing system performance in various dimensions. Deep learning is an important instrument for future developments in FSO systems because of its capacity to handle complicated patterns and adjust to shifting circumstances. Numerous prior studies have explored the application of deep learning to enhance visual communications [1]. Study, for instance, discovered that integrating convolutional neural networks with existing demodulation and error correction systems can enhance detection accuracy over threshold classification schemes. To achieve low complexity, reduced modeling difficulties, high accuracy, and discriminability [4]. Research establishes data-driven channel modeling methods for deep learning in free-space optical communication systems. Using generative adversarial network (GAN), bidirectional long short-term memory (BiLSTM), and Bayesian neural network (BNN) DL techniques, he created an FSO channel. As a result, a comprehensive comparison of their performance concerning data distribution, fitted probability density functions, Kullback-Leibler (KL) divergence, optical amplitude waveforms, and 95% confidence interval was performed. The results show the optimal performance of the GAN-based channel, indicating that it is suitable for learning a random FSO channel. Using thermal nonlinearities exhibited by atomic media [5].

The results indicate that the GAN-based communication channel demonstrates optimal performance, confirming its suitability for learning a random FSO channel using thermal nonlinearity in atomic media, relying on temperature-dependent refractive index variations to generate the nonlinear optical processes essential for neural network computations.

The three main subsystems of FSOC system block.

Diagram is the transmitter, channel, and receiver. Figure 1 show the FSOC block diagram.

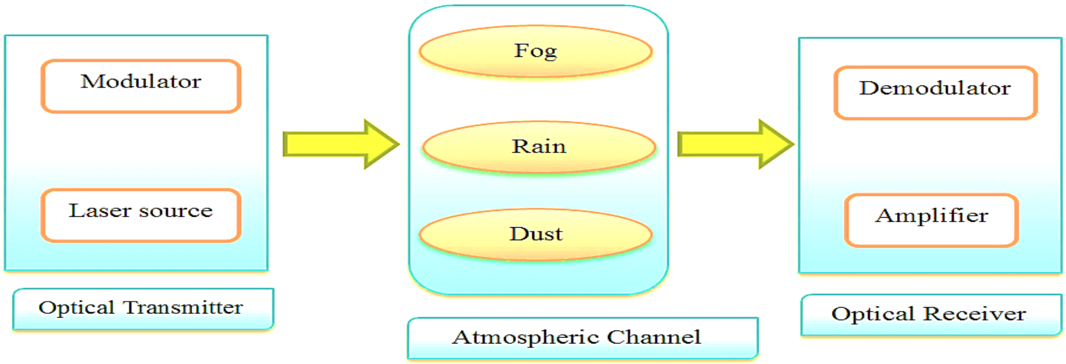

Fig. (1): The FSOC block diagram

- **Transmitter**: The primary function of this device is to encode an incoming message signal onto an optical carrier for transmission to the receiver through the surrounding environment. A transmitting telescope or optical antenna, an optical source - likely a laser diode—and the modulator are required components. The telescope's moving component performs both beam tracking and beam shaping. [6]

- **Channel:** Since erratic weather conditions like dust, fog and rain, can impact the received signal's power, making the channel a major FSOC limiting factor. It is crucial to note that these variables change greatly over time and do not have fixed properties. [6]
- **Receiver:** Recovering the transferred data is done using a receiver. It is composed of a demodulator, an extremely sharp optical band pass filter to cut down on background noise, and a receiver telescope such as an avalanche photodiode (APD) and, (PIN) photodiode the equivalent of a transmitting telescope. That is equivalent to the transmitter telescope. [7] An optical transmitter is used to transmit the collimated light beam. The transmitted beam widens as the linkage distance increases. The bigger beam width reasons signal loss, a drop in signal-to-noise ratio (SNR), and an increase in bit error rate (BER) by decreasing the connection margin at the receiver side. To receive all of the information supplied by the optical carrier, the receiving side's receiver aperture diameter should be larger, but doing so also increases noise from ambient light. [8]. The ratio of the receiving power (P_r) to the receiver threshold or sensitivity (S), which is frequently expressed in dB, is known as the link margin (P_l). An additional link margin must be employed to counteract the power loss. [9]

$$p_l = \frac{10 log p_r}{S} \qquad (1)$$

For actual recovery at the receiver side, the average power of the signal must be greater than the receiver sensitivity. [10]

Rain Attenuation

Raindrop size distribution models are crucial in rainfall modeling, with the Marshall-Palmer model being the most well-known due to its impact on signal attenuation.

Attenuation is calculated as follows and represented in dB/km:

$$Att_{rain} = k_1 R^{k_2} \qquad (2)$$

Where:

R= rain rate in mm/hr.

K_1 and K_2 = model characteristics that are dependent on the temperature and size of the raindrops. The rain attenuation prediction model settings for FSO that are advised are $k1$ = 1.074 and $k2$ = 0.67, in that order. Table 1 displays the value of *R* for various rain circumstances. [11]

Table 1. R Values in the Event of Rain [11].

Rainfall	R Values (*mm / hr*)
Light rain	(2.5)
Medium rain	(12.5)
Heavy rain	(25)
Cloud burst & heavy rain	(100)

Fog Attenuation

To forecast the optical attenuation statistics from the visibility data, a relationship needs to be made, the attenuation increases to more than 350 dB when visibility is less than 50 meters. Fog is the primary cause of atmospheric attenuation since it has an impact on both scattering and absorption.

In this instance, stronger lasers and certain techniques are needed to enhance communication. [12] Different models are used to calculate the attenuation caused by fog and dust, based on the origin of an empirical model and a theoretical approach that depends on the visibility range. As in the following equation:

$$\alpha = \frac{3.91}{V} \left(\frac{550}{\lambda}\right)^{q} \qquad (3)$$

Where λ is the wavelength in nanometers and V is the visible range in kilometers. The particle size distribution is given by ***q, α*** which stands for the overall attenuation coefficient. The relationship between the particle size distribution and the visibility range can be explained using the Kruse model. [13]

$$q = \begin{cases} 1.6 & if\ V > 50km \\ 1.3 & if\ 6\ km < V < 50\ km \\ 0.585V^{1/3} & if\ V < 6\ km \end{cases} \qquad (4)$$

According to Eq. (4), greater wavelengths will experience less attenuation in any weather. Kim modified Eq. (4) to account for low visibility. Consequentially, the Kim model's particle size can be expressed as follows. [13]

$$q = \begin{cases} 1.6 & if\ V > 50km \\ 1.3 & if\ 6\ km < V < 50\ km \\ 0.16V + 0.34 & if\ 1\ km < V < 6\ km \\ V - 0.5 & if 0.5\ km < V < 1\ km \\ 0 & if\ V < 0.5\ km \end{cases} \qquad (5)$$

Dust Attenuation

Based on the range of sight, dust occurrences can be divided into four categories: dust storms (moderate dust), gusting dust (light dust), dust haze (light dust), and severe dust storms (dense dust). Consequently, Table 2 divides dust storms into four types based on visibility range, and the following formula is used to determine visibility range V [14]:

$$V = -\frac{10logT_{th}}{\alpha}(Km) \qquad (6)$$

Where T_{th}: contrast threshold= ***0.02*** according to Koschmieder law. The signal attenuation coefficient ***α*** is calculated as follows [14]:

$$\alpha = -\frac{10logT}{4.343L}(dB/Km) \qquad (7)$$

T is the transmittance of the optical signal at 550 nanometers, and ***L*** is the connection length in kilometers.

Table 2. Dusty storms based on the range of visibility [15].

Dust type	Visibility (km)	Description
Extreme dust storm	< 0.2	Dense

Dust storm	0.2-1	Moderate
Haze dust	≤ 10	Light
Blowing dust	1-10	Light

Neural Networks

The application of machine learning to optical communications is a new field that will soon get greater attention. A trained algorithm can evaluate and comprehend data with the help of a wide range of tools included in machine learning ML algorithms can be broadly classified into two classes: supervised and unsupervised. When training supervised learning algorithms, labeled examples such as inputs for which the output is known are used. Unsupervised

Algorithms, on the other hand, do not presuppose a known outcome for a given set of input values [16]. Multiple layers of neurons make up a typical deep neural network. Every neuron in the preceding layer gets input signals, except for those in the first layer. Except for batch normalization, the neuron multiplies the total of the signals by weights that can be adjusted before performing a nonlinear operation, the output of which is then used as an input signal by one or more neurons in the layer below. There are numerous neural network design variations available, as well as various training techniques tailored to particular use cases. A set of training data and matching labels are given to the network for a standard supervised learning picture classification task. The network can change the weights progressively until they converge on an ideal solution by continuously comparing the output result against the labels. By repeatedly comparing the output result against the labels, the network can gradually adjust its weights until the weights converge on an optimum solution. [5]

The FSO channel requires a special modeling algorithm because, in contrast to fiber channels and RF channels, it has distinct characteristics and effects related to the interaction of the carrier with the atmosphere. Consequently, considering the mechanical characteristics and performance, it is crucial to carry out a thorough and meticulous examination of the optimal DL technique for modeling the FSO channel. Figure 2 illustrates a free-space optical communication system schematic and a data-driven channel model based on deep learning concepts. [4]

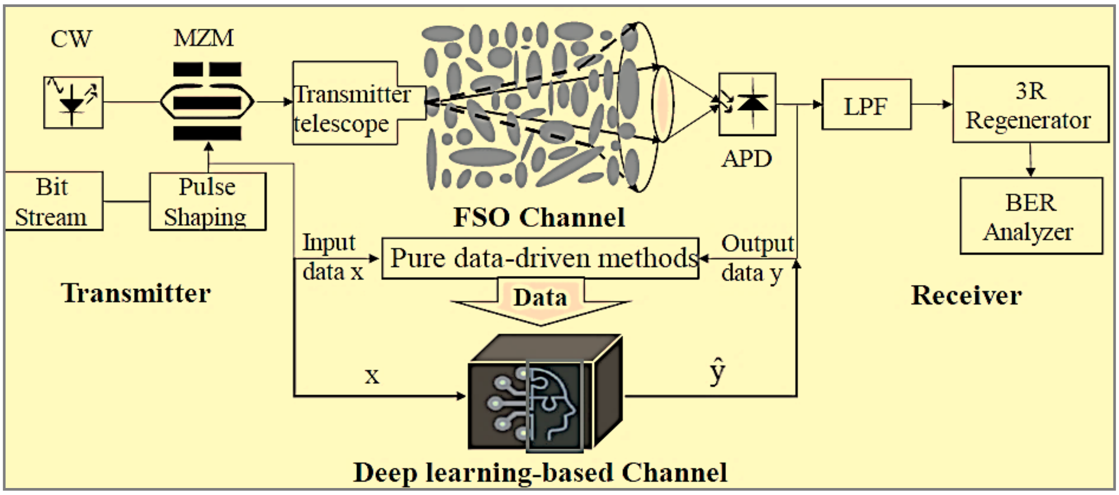

Fig. (2): Diagram of a data-driven channel model using free-space optical communication systems and deep learning principles (MZM: Mach-Zehnder Modulator, CW: Continuous wave, and LPF: Low-pass filter) [4]

To understand the architecture of the convolutional neural network CNN, Figure 3 depicts a CNN example; it includes mathematical representations of four inputs, four outputs, and their synaptic connections. The input nodes of the CNN receive input signals, which are subsequently sent to the output nodes via synaptic connections for processing, resulting in the output. Mathematical models that give each synaptic connection a weight are used to model the strengths of the connections [16].

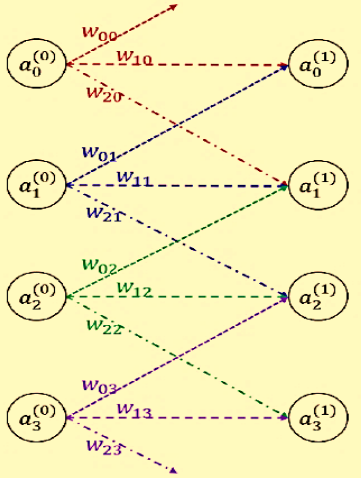

$$a_1^{(1)} = \sigma(w_{20}\, a_0^{(0)} + w_{11}\, a_1^{(0)} + w_{02}\, a_2^{(0)} + b_1)$$

$$a_2^{(1)} = \sigma(w_{21}\, a_1^{(0)} + w_{12}\, a_2^{(0)} + w_{03}\, a_3^{(0)} + b_2)$$

$$a_i^{(l)} = \sigma\left(\sum_{m=0}^{N_m-1} w_{m,\mathrm{k-m}}\, a_{k-m}^{(l-1)} + b_i\right)$$

$$\begin{cases} k = i + \dfrac{(N_m - 1)}{2} \\ w_{m,k-m} = 0 \; if \; k - m < 0 \; or \; \mathrm{k} - m \geq N \end{cases}$$

Fig. (3): Example of a simple CNN with corresponding mathematical formula $a_i^{(l)}$ represents the *i*-th input or output node in the *l*-th layer; w_{ij} indicates the weight connecting the *j*-th input node and the *i*-th output node; b_i is the *i*-th bias; *N* is the size of the input array; N_m is the number of weights connected to an input/output or the size of a kernel; and σ is a sigmoid function [16].

Simulation Part

The ideal power level is produced by entering data into MATLAB software, such as wavelength, power, and distance. One hidden layer of ten neurons is used to form a basic feed-forward neural network. The training data was also used to train the network. The data was split up into test, validation, and training sets. Next, the trained network is put to the test using the test data, and its effectiveness is assessed. In the end, a chart was made to contrast the numbers predicted by the neural network with the actual boost energy.

Figure 4 Shows the CNN simulation diagram.

Describe the neural network's architecture:

Input: The number of features in your data (in this case, four features total—distance, atmospheric conditions, input power, and wavelength) equals the number of neurons in the input layer.

Hidden Layers: Two hidden layers with ten neural units per layer have been defined here, where w refers to the weight of the vector and b to the bias.

Output: The expected enhanced power is represented by a single neural unit in the output layer.

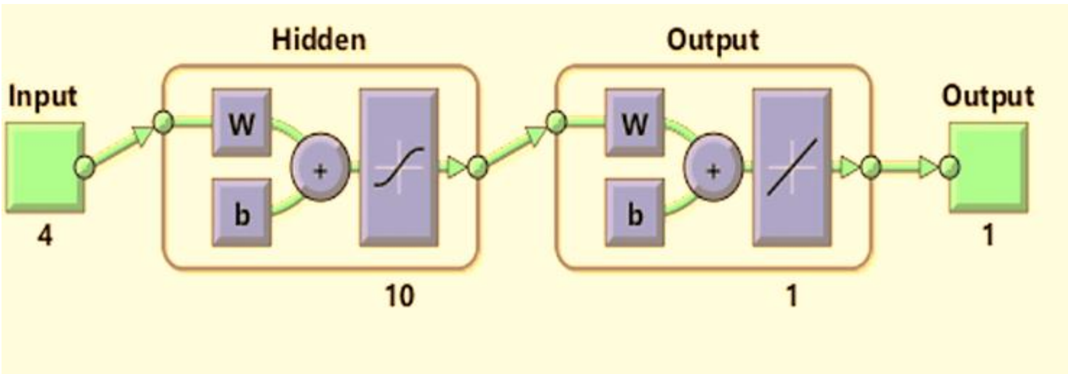

Fig. (4): The CNN simulation diagram.

Results and Discussion

Following the development and execution of a MATLAB program to design and train a neural network for power optimization in a free-form optical communications system (FSO), the outcomes will be reviewed in terms of the neural network's performance, as well as the graphs that were produced to examine it. The values of the iteration count and the level of neural network improvement are displayed in Figure 5.

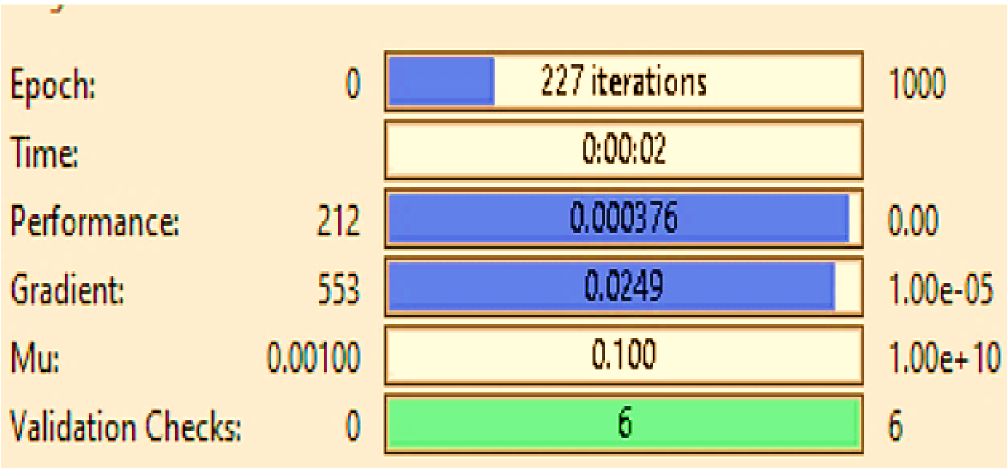

Fig. (5): The number of iteration values and the level of neural network improvement

The performance metric mean square error (MSE), which indicates how accurately the neural network predicts the optimal power, was acquired after the program was executed. A lower MSE value indicates better performance. A low mean square error (MSE) indicates that the neural network has learned effectively from the training set and can predict with increased ability with high accuracy. The following code produces a graph that compares the actual boosted power to the improved power that the neural network predicted. Figure 6 refers to the mean square error of the improved ability.

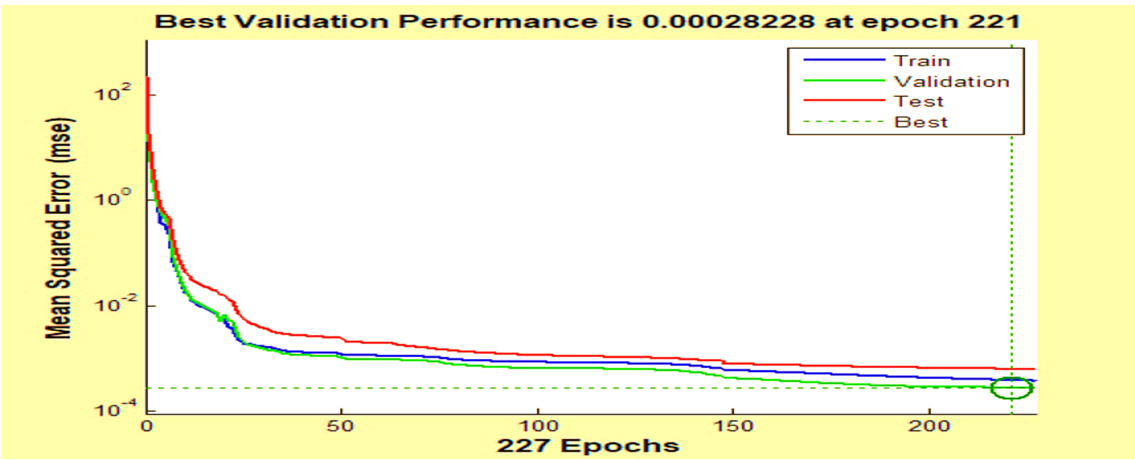

Fig.6 The mean square error of the improved ability

A low MSE indicates that the neural network has effectively learned and can accurately predict performance.

The resulting graph illustrates the comparison between the actual enhanced power and the power predicted by the neural network.

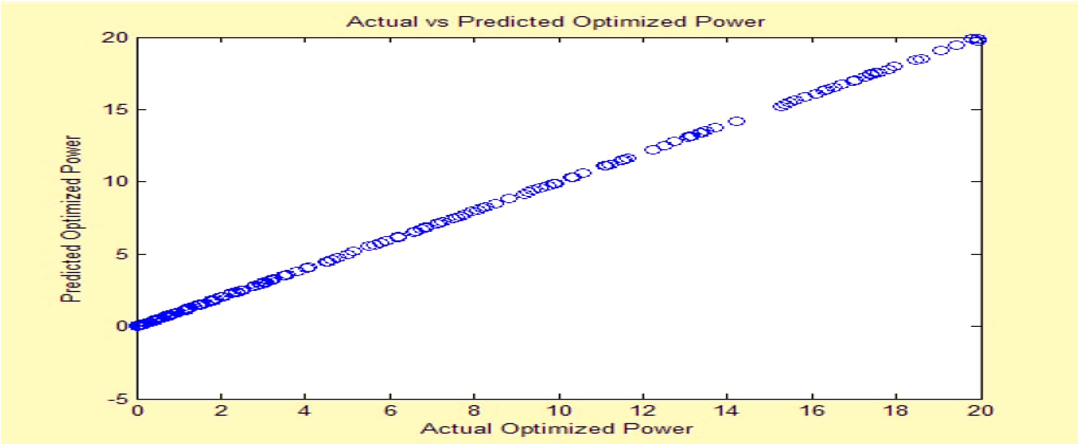

Fig. (7): The real enhanced power versus the improved power predicted by the neural network

Figure 7 above compares actual and predicted values of improved capacity. If the points are close to the straight line y = x, the predictions are accurate. The large dispersion of points away from the line y = x designates that the model needs additional improvement. The network is trained using training data. The data is divided into training, validation, and test groups. The trained network is tested on test data, and performance is measured. Finally, a chart is created to compare the actual enhanced energy with the values predicted by the neural network. Figure 8 shows the Actual enhanced energy with the values predicted

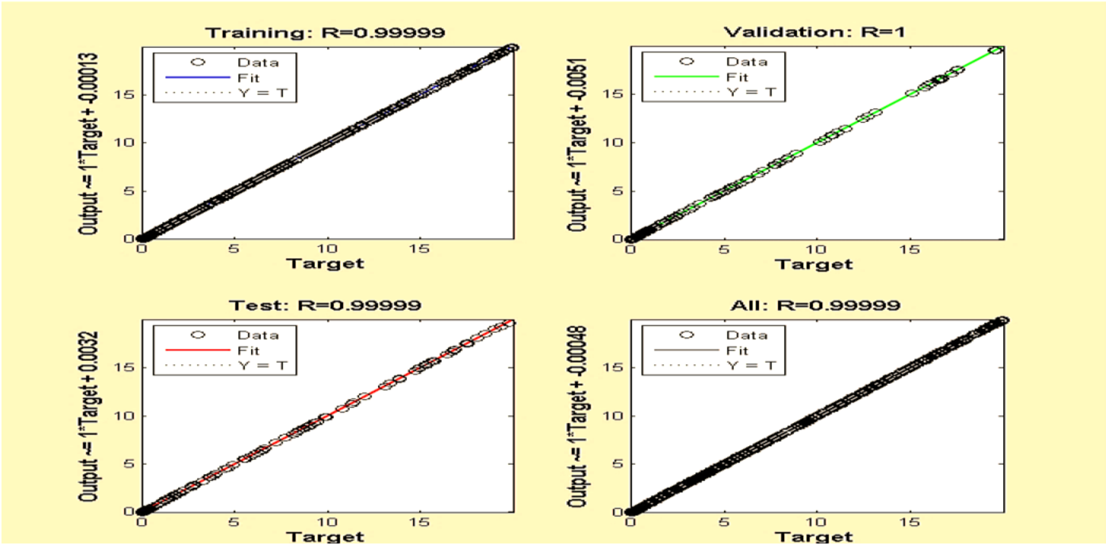

Fig. (8): Actual enhanced energy with the values predicted by the neural network (Training, testing, and visualization)

The network is trained using training data. The data is divided into training, validation, and test sets. The trained network is tested on test data, and performance is measured. Finally, a chart is created to compare the actual enhanced energy with the values predicted by the neural network. Figure 9 shows increasing the number of training cycles (epochs) to improve model accuracy. where (epochs) refers to the number of cycles in which the entire training dataset passes through the neural network.

In other words, each epoch represents one pass through all the data samples in the training set, where the data is passed through the neural network forward and then the weights are updated as the information is passed backward.

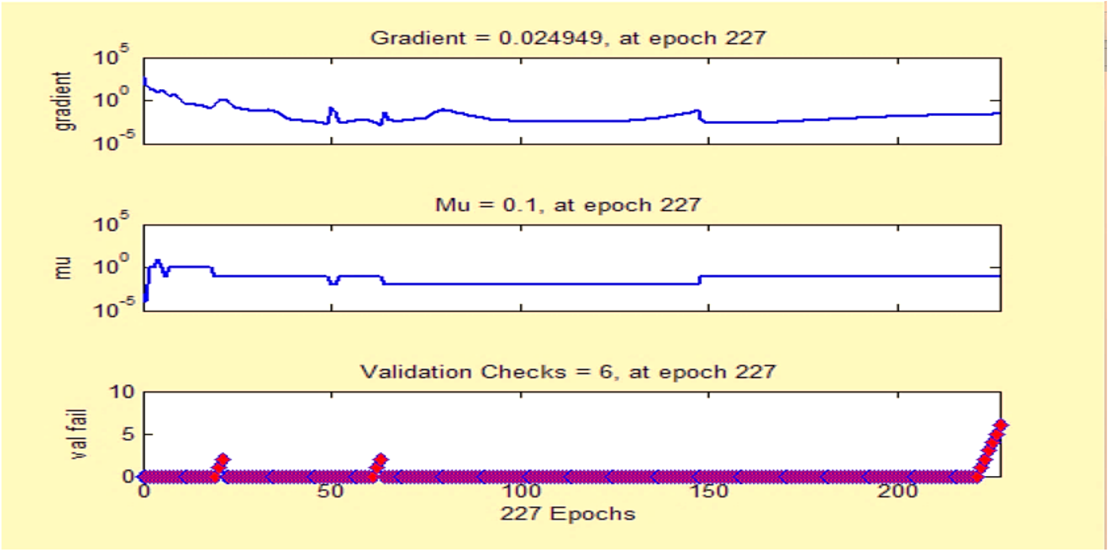

Fig. 9 Increase model accuracy, and increase the number of training cycles, (epochs).

In Figure 10, the autocorrelation of an error time series is shown. The autocorrelation function quantifies the relationship between errors over various time intervals. When autocorrelation levels are high, it means that there is a persistent systematic pattern in the data or model, implying that the errors are not independent.

Since autocorrelation values are random and unaffected by previous values, we would anticipate a sharp decline in these values. This indicates that, in optimizing free-space optical communications systems, the neural network is successfully detecting and adjusting for fluctuations brought on by elements like atmospheric turbulence.

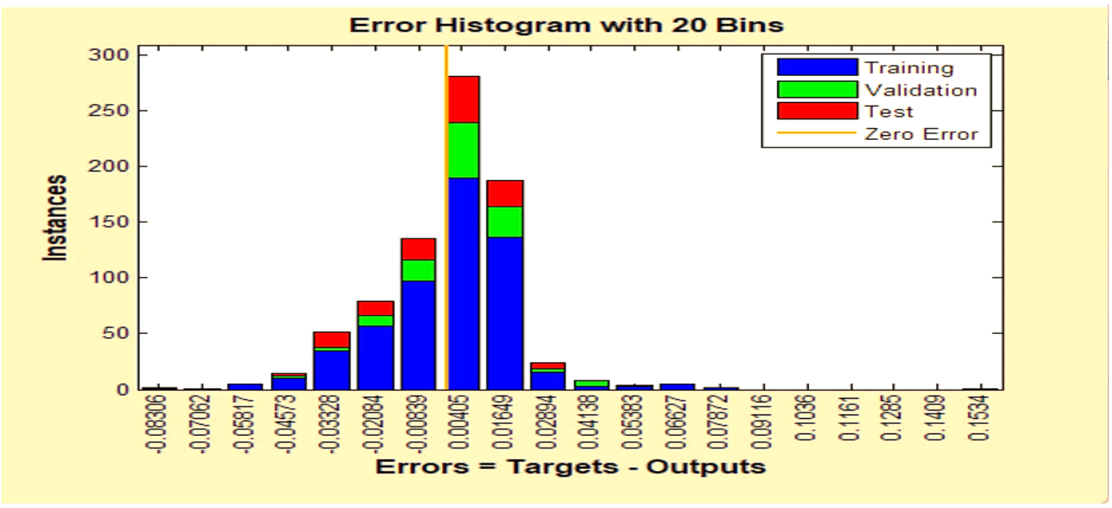

Fig. (1):0 The autocorrelation of the error time series

Conclusion

Based on the results obtained, we may make some significant inferences after setting up and executing a MATLAB program to build a neural network for power optimization in a free-form optical communication system (FSO).

The main points Neural network performance:

Mean Square Error (MSE): A low value of MSE indicates that the neural network is able to predict the improved ability with high accuracy. This shows that the model has learned well from the training data.

Actual vs. predicted power: The graph displays a comparison between actual and predicted values of optimized power. If the points are close to the straight line y = x, this designates that the predictions are accurate.

Dispersion: A large dispersion of points away from the y = x line designates that the model needs additional improvement.

Neural network structure: Number of hidden layers: Using two hidden layers, each containing 10 neurons, was sufficient in this research.

Input and Output: The input layer contains 4 features (distance, weather conditions, input power, wavelength), while the output layer contains one neural unit to represent the predicted enhanced power.

Conflict of Interest:

The authors declared no conflict of interest.

References

[1] Ali, M. A. A., Baqi, Z. H., & Rahi, S. K. (2020). On the performance of free space optical communication link over dust environment. AIP Conference Proceedings, 2213, 020105.

[2] Amirabadi, M. A., Kahaei, M. H., & Nezamalhosseni, S. A. (2021). Low complexity deep learning algorithms for compensating atmospheric turbulence in the free space optical communication system. IET Opotelectron.–105.Journal, Volume 16 (93), PP 1-13.

[3] Anuranjana, Kaur, S., & Goyal, R. (2019). Analysis of Terrestrial FSO Link Performance Considering Different Fog Conditions and Internal Parameters of the System. 6th International Conference on Signal Processing and Integrated Networks (SPIN), PP 552-557.

[4] Bart, M. P., Savino, N. J., Regmi, P., Cohen, L., Safavi, H., Shaw, H. C., Lohani, S., Searles, T. A., Kirby, B. T., Lee, H., & Glasser, R. T. (2022). Deep learning for enhanced free-space optical communications. Journal of Optical Communications and Networking, PP 1-7.

[5] Chen, W., Zhang, M., Wang, D., Zhan, Y., Cai, S., Yang, H., Zhang, Z., Chen, X., & Wang, D. (2023). Deep learning-based channel modeling for free space optical communications. *Journal of Lightwave Technology*, *41*(1), 183–198.

[6] Dulamjav, D., & Zundui, B. (2022). The Analysis of FSO Link Performance in Ulaanbaatar. [ICTFocus Journal], Volume 1(1)], PP 47-54.

[7] Hassan, M. M., & Rather, G. M. (2020). Free space optics (FSO): A promising solution to first and last mile connectivity (FLMC) in the communication networks. Wireless and Microwave Technologies Journal, Volume 4, PP1-15.

[8] Ju, Y.-G. (2023). Scalable optical convolutional neural networks based on free-space optics using lens arrays and a spatial light modulator. J. Imaging, 9(11), 241.

[9] Kaymak, Y., Rojas-Cessa, R., Feng, J., Ansari, N., Zhou, M., & Zhang, T. (2018). A survey on acquisition, tracking, and pointing mechanisms for mobile free-space optical communications. IEEE, PP1-21.

[10] Khalil, H., Qamar, F., Shahzadi, R., Ali, M., Nadeem, M. F., Qamar, N., & Sajjad, I. A. (2020). FSO Communication: Benefits, Challenges, and its Analysis in DWDM Communication System. [Sir Syed University Research Journal of Engineering and Technology], PP 45-53.

[11] Lionis, A., Peppas, K., Nistazakis, H. E., Tsigopoulos, A., Cohn, K., & Zagouras, A. (2021). Using Machine Learning Algorithms for Accurate Received Optical Power Prediction of an FSO Link over a Maritime Environment. Photonics Journal, Volume 8(212)], PP 1-17.

[12] Minhas, A. A., Khan, M. S., Henna, S., & Iqbal, M. S. (2021). Attenuation-based hybrid RF/FSO link using soft switching. Optical Engineering Journal, Volume 60(5), PP 1-22.

[13] Mushtaq, M. T., Yasir, S. M., Khan, M. S., Wahid, A., & Iqbal, M. S. (2018). Analysis of internal design parameters to minimize geometrical losses in free-space optical

communication link. International Advances in Applied Physics and Materials Science (APMAS) Journal, Volume 134 (1), PP 275-278.

[14] Ryou, A., Whitehead, J., Zhelyeznyakov, M., Anderson, P., Keskin, C., Bajcsy, M., & Majumdar, A. (2021). Free-space optical neural network based on thermal atomic nonlinearity. Photonics Research Journal, Volume 9 (4)], PP 128-134.

[15] Shaker, F. K., Aliy, M. A. A., & Ameer, F. S. A. A. (2019). Utilization of MIMO Concept for Optical Communication System under Fog Condition. Ecti Transactions on Electrical Eng., Electronics, and Communications journal, [Volume 17(2), PP 130-135.

[16] Wang, M., Guo, W., & Yuan, X. (2021). Single-shot wavefront sensing with deep neural networks for free-space optical communications. Optics Express Journa Vol. 29, (3), PP 1-14.